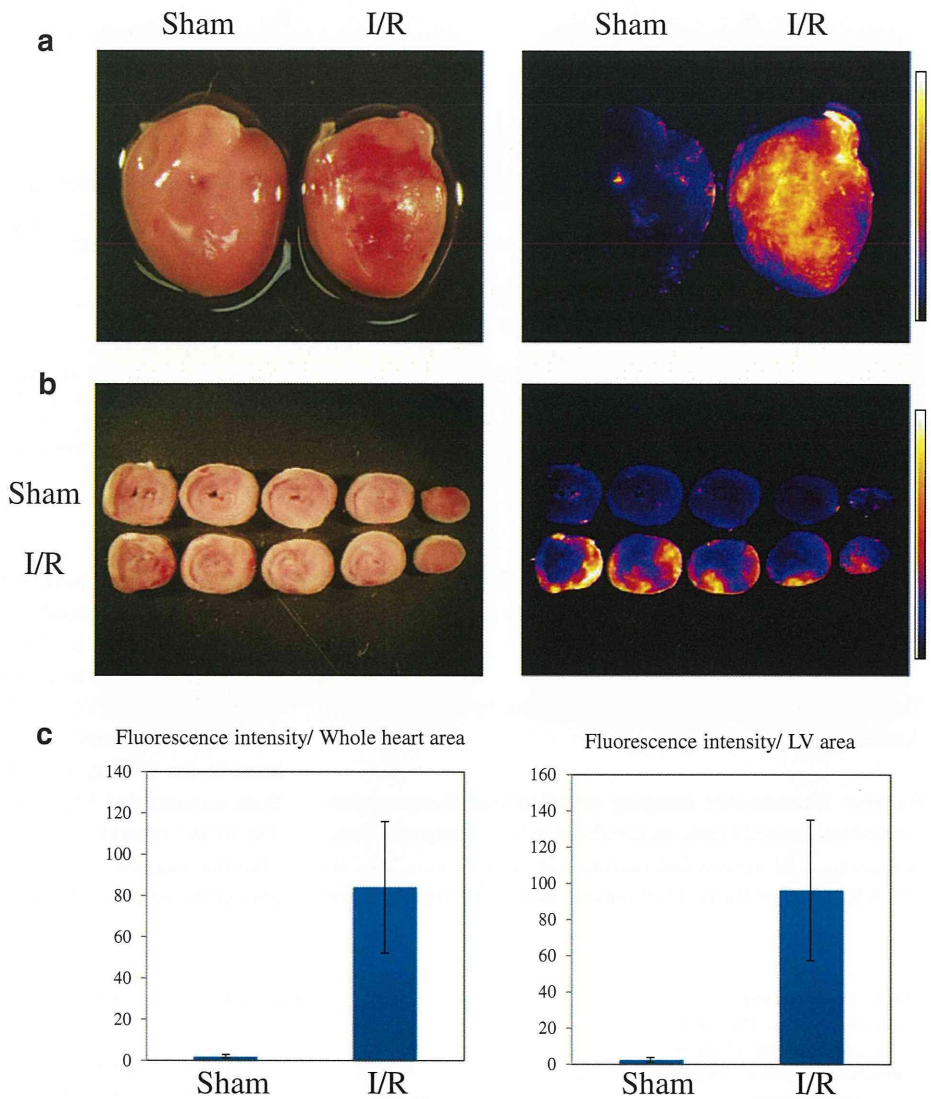

Fig. 2 Representative pictures of ischemia/reperfused myocardium with and without fluorescence-labeled nano-sized beads. Representative pictures obtained by fluorescent imaging are shown in **a** (*whole heart*) and **b** (*sliced hearts*). Quantitative analysis revealed that the average fluorescence intensity of the whole heart (**c** *left*) or the left ventricle (**c** *right*) of the I/R hearts was significantly higher than that of the sham-operated hearts

accumulation of nano-sized beads was observed in the I/R myocardium, 3) liposomal amiodarone showed a smaller reduction in the HR and systolic BP compared with free amiodarone, and 4) liposomal amiodarone, but not amiodarone, reduced the VT/VF duration and mortality during the reperfusion period compared with saline.

Table 2 Amiodarone concentration in the blood and I/R myocardium

Groups	Plasma, ng/mL	Myocardium, ng/mL
Saline	N.D.	N.D.
Free amiodarone	472±147	N.D.
Liposomal amiodarone	3872±378*	71±7*

Data are expressed as the mean ± SEM. *N.D.* not detected. $n=3$ rats in each group. * $p<0.05$ versus free amiodarone

Preparation of Liposomal Amiodarone

This study is the first to encapsulate amiodarone in PEGylated liposomes, although it has been previously encapsulated in other liposomes [22] and micelles [23]. We demonstrated that lipid bilayers composed of unsaturated lipids are more suitable for encapsulating amiodarone in PEGylated liposomes compared with those composed of saturated lipids. PEGylated liposomes have a long circulating time in the bloodstream because PEG endows a steric barrier to liposomes, allowing them to avoid interactions with opsonins and cells of the mononuclear phagocytic system [24]. Thus, they have been used to increase drug stability, safety, and bioavailability in clinical applications. In this study, we found that a higher concentration of amiodarone was retained in the blood when we administered liposomal amiodarone compared with the administration of

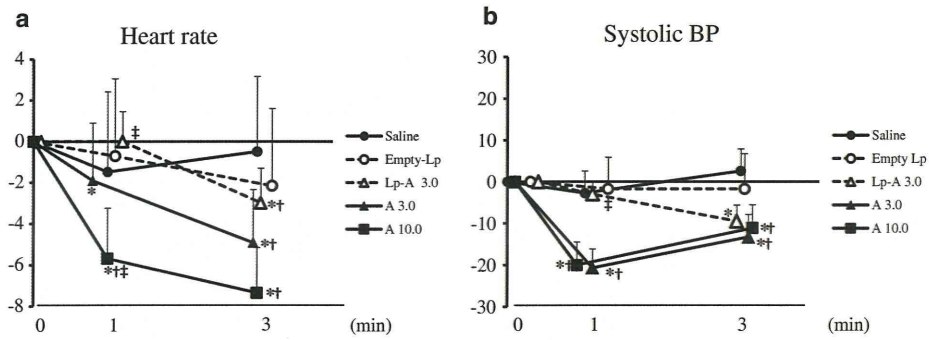

Fig. 3 Time-course changes in HR and systolic BP after drug administration. Shows the percent change from baseline for HR (**a**) and systolic BP (**b**) after intravenous administration of the tested drugs. The data are expressed as the mean ± SEM. *$P<0.05$ versus baseline, paired t-test. $P=0.0009$ (HR), 0.0002 (systolic BP) between amiodarone (3 mg/kg) and liposomal amiodarone (3 mg/kg), 1-way repeated-measurement ANOVA. †$P<0.05$ versus saline, ‡$P<0.05$ versus amiodarone (3 mg/kg), 1-way repeated-measurement ANOVA with Bonferroni's multiple comparison

free amiodarone, suggesting that encapsulation of amiodarone in PEGylated liposomes enhances the stability of amiodarone in the blood.

Targeted Delivery to the I/R Myocardium by Liposomal Amiodarone

Ex vivo fluorescence imaging revealed that fluorescence-labeled nano-sized beads accumulated in the I/R myocardium, suggesting that myocardial permeability can be enhanced in the I/R myocardium. Consistent with this finding, we observed that the amiodarone concentration in the I/R myocardium in the liposomal amiodarone group was much higher compared with that in the amiodarone group. Enhanced permeability in the I/R myocardium and the prolonged presence of amiodarone in PEGylated liposomes in the blood represent a possible mechanism for increased amiodarone concentrations in the I/R myocardium. Amiodarone will be released from accumulated liposomal amiodarone in I/R myocardium due to the natural decay and concentration gradient. These findings suggest that the I/R myocardium is a promising passive target for liposomal drug delivery.

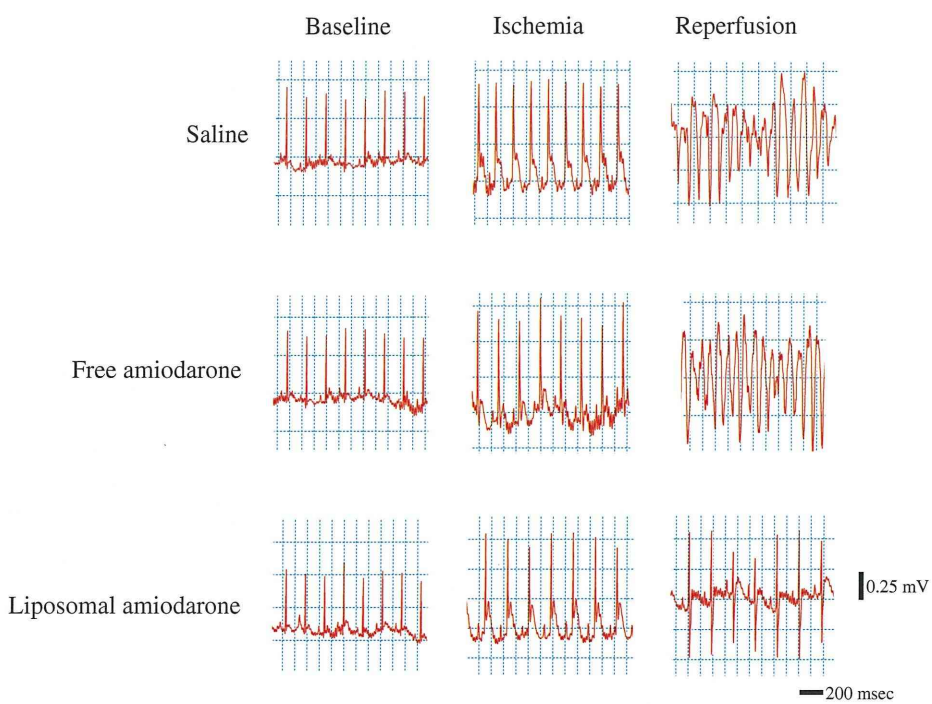

Fig. 4 Representative electrocardiograms. The *upper, middle and lower panels* show representative electrocardiograms under baseline conditions during ischemia and at the onset of reperfusion for rats that received saline, free amiodarone (3 mg/kg) and liposomal amiodarone (3 mg/kg), respectively

Table 3 Lethal arrhythmias and mortality in an I/R rat model

	Number	VT/VF duration (sec)	Mortality (%)
Saline	7	195±42	71
Empty liposomes	6	162±31	50
Amiodarone (3 mg/kg)	6	167±78	33
Amiodarone (10 mg/kg)	6	36±12*	0#
Liposomal Amiodarone (3 mg/kg)	6	18±9*	0#

*$p<0.05$ versus saline (VT/VF duration). # $p<0.05$ versus saline group (mortality). *VT* ventricular tachycardia, *VF* ventricular fibrillation

Minimal Negative Hemodynamic Effects of Liposomal Amiodarone

Amiodarone causes hypotension and bradycardia in clinical settings [4, 5]. In this study, both free and liposomal amiodarone significantly reduced the HR and systolic BP; however, the time-course changes for both the HR and systolic BP in the liposomal amiodarone group were significantly smaller compared with those following the corresponding dose of free amiodarone. Importantly, the reductions in HR and systolic BP at 1, but not 3, minutes after liposomal amiodarone administration were significantly smaller compared with those following the corresponding dose of amiodarone. These findings suggest that liposomal amiodarone may minimize the negative effects on systemic hemodynamics immediately after the administration of amiodarone. One possible mechanism to explain this finding is that amiodarone on the surface of the liposome membrane is covered with PEG so that amiodarone cannot act directly on cardiovascular cells. Gradual release of amiodarone from liposome may minimize the rapid hemodynamic changes, because systemic hemodynamic effects of liposomal amiodarone were significantly attenuated in liposomal amiodarone group than free amiodarone group.

Augmented Anti-arrhythmic Effects of Liposomal Amiodarone

In this study, liposomal amiodarone (3 mg/kg), but not the corresponding dose of free amiodarone (3 mg/kg), significantly reduced the VT/VF duration and mortality compared with saline in an I/R rat model. Because the acute effects of amiodarone are known to be attributable to blockade of Na^+, Ca^{2+} and dose-dependent K^+ channels [2, 25], increasing the concentration of amiodarone in the I/R myocardium may augment its anti-arrhythmic effects through its tonic effects on cardiomyocytes caused by blocking cardiac ionic currents. Kishida et al. reported that amiodarone enhances nitric oxide production in cultured human endothelial cells [26]. Furthermore, amiodarone protects cardiac myocytes against oxidative injury by scavenging free radicals [27]. These pleiotropic effects of amiodarone are also enhanced by its increased concentration in the I/R myocardium via PEGylated liposomes, which may contribute to the reduction of lethal arrhythmias during reperfusion followed by ischemia. In the present study, since we did not do any procedure such as electrical conversion or cardiac massage for VT/VF, the mortality was higher than in our previous report [16].

Clinical Implications

In clinical settings, higher doses of amiodarone cause hypotension and non-cardiac death or induce worsening heart failure through negative inotropic effects [28]. These effects often diminish the beneficial effects of amiodarone for patients with AMI or heart failure [8, 9]. The present study demonstrated that liposomal amiodarone (3 mg/kg) exerts anti-arrhythmic effects similar to a high dose of free amiodarone (10 mg/kg) while reducing the extent of bradycardia and hypotension, suggesting that encapsulating amiodarone in liposomes augments its anti-arrhythmic effects and reduces its negative effects on hemodynamic parameters with reducing administrative dose. These findings can have a great impact on preventing lethal arrhythmias during reperfusion in AMI patients.

Study Limitations

There are several limitations in this study. We used a brief period of I/R without myocardial infarction in rats. Sakamoto et al. demonstrated that the incidence of VT/VF in a rodent model was 'bell-shaped' with a maximum at 5 min of ischemia and that most lethal arrhythmias occurred within first 20 s after the onset of reperfusion [29]. Consistently, our data showed that the mean time at which the lethal arrhythmia occurred after the onset of reperfusion was 3.3+/−1.6 s. Therefore, we chose the 5 min of ischemia followed by 15 min of reperfusion model. We also chose the timing of drug administration before the onset of ischemia to clarify whether liposomal-amiodarone could prevent the lethal arrhythmia that occurs in the early period of reperfusion. In addition, in clinical practice lethal arrhythmias often occur after a brief period of I/R without any irreversible damage to the heart, indicating that the anti-arrhythmic effects of liposomal amiodarone during a brief period of ischemia model could have clinical relevance [30]. However, careful interpretation is necessary when using liposomal amiodarone in acute myocardial infarction with irreversible damage to confirm the beneficial effects of liposomal amiodarone. Furthermore, because the electrophysiology of rats differs from that of humans and drug administration in our study started before the onset of

ischemia, additional pre-clinical studies including a longer period of I/R model to consider the timing of drug administration are needed using large animal models. We should also take into account that the potential side effects of amiodarone such as bradycardia are minimal in the left coronary artery occlusion model used in the present study.

Conclusion

In conclusion, the targeted delivery of liposomal amiodarone to the I/R myocardium exerted strong anti-arrhythmic effects and reduced the negative impact on systemic hemodynamics. Nano-sized liposomes may be a promising drug delivery system for targeting the I/R myocardium with cardioprotective agents.

Acknowledgments The authors thank Takaki Hayakawa for her technical assistance, Takeshi Aiba for his special advice about data analysis. This research was supported by Grants-in-Aid from the Ministry of Health, Labor, and Welfare of Japan; Grants-in-Aid from the Ministry of Education, Culture, Sports, Science, and Technology of Japan; grants from the Japan Heart Foundation; and grants from the Japan Cardiovascular Research Foundation.

References

1. Di Diego JM, Antzelevitch C. Ischemic ventricular arrhythmias: experimental models and their clinical relevance. Hear Rhythm. 2011;8:1963–8.
2. Kodama I, Kamiya K, Toyama J. Cellular electropharmacology of amiodarone. Cardiovasc Res. 1997;35:13–29.
3. Vassallo P, Trohman RG. Prescribing amiodarone: an evidence-based review of clinical indications. JAMA. 2007;298:1312–22.
4. Scheinman MM, Levine JH, Cannom DS, et al. Dose-ranging study of intravenous amiodarone in patients life-threatening ventricular tachyarrhythmias. The Intravenous Amiodarone Muticenter Investigators Group. Circulation. 1995;92:3264–72.
5. Podrid PJ. Amiodarone; reevaluation of an old drug. Ann Intern Med. 1995;122:689–700.
6. Shiga T, Tanaka T, Irie S, Hagiwara N, Kasanuki H. Pharmacokinetics of intravenous amiodarone and its electrocardiographic effects on healthy Japanese subjects. Hear Vessel. 2011;26:274–81.
7. Wenzel V, Russo SG, Arntz HR, et al. [Comments on the 2010 guidelines on cardiopulmonary resuscitation of the European Resuscitation Council.]. Anaesthesist. 2010.
8. Elizari MV, Martínez JM, Belziti C, et al. Morbidity and mortality following early administration of amiodarone in acute myocardial infarction. GEMICA study investigators, GEMA Group, Buenos Aires, Argentina. Grupo de Estudios Multicentricos en Argentina. Eur Heart J. 2000;21:198–205.
9. Hu K, Gaudron P, Ertl G. Effects of high- and low-dose amiodarone on mortality, left ventricular remodeling, and hemodynamics in rats with experimental myocardial infarction. J Cardiovasc Pharmacol. 2004;44:627–30.
10. Semalty A, Semalty M, Rawat BS, Singh D, Rawat MS. Pharmacosomes: the lipid-based new drug delivery system. Expert Opin Drug Deliv. 2009;6:599–612.
11. Whitehead KA, Langer R, Anderson DG. Knocking down barriers: advances in siRNA delivery. Nat Rev Drug Discov. 2009;8:129–38.
12. Malam Y, Loizidou M, Seifalian AM. Liposomes and nanoparticles: nanosized vehicles for drug delivery in cancer. Trends Pharmacol Sci. 2009;30:592–9.
13. Horwitz LD, Kaufman D, Keller MW, Kong Y. Time course of coronary endothelial healing after injury due to ischemia and reperfusion. Circulation. 1994;90:2439–47.
14. Dauber IM, VanBenthuysen KM, McMurtry IF, et al. Functional coronary microvascular injury evident as increased permeability due to brief ischemia and reperfusion. Circ Res. 1990;66:986–98.
15. Galagudza MM, Korolev DV, Sonin DL, et al. Targeted drug delivery into reversibly injured myocardium with silica nanoparticles: surface functionalization, natural biodistribution, and acute toxicity. Int J Nanomedicine. 2010;5:231–7.
16. Takahama H, Minamino T, Asanuma H, et al. Prolonged targeting of ischemic/reperfused myocardium by liposomal adenosine augments cardioprotection in rats. J Am Coll Cardiol. 2009;53:709–17.
17. Riva E, Hearse DJ. Anti-arrhythmic effects of amiodarone and desethylamiodarone on malignant ventricular arrhythmias arising as a consequence of ischaemia and reperfusion in the anaesthetised rat. Cardiovasc Res. 1989;23:331–9.
18. Canyon SJ, Dobson GP. Protection against ventricular arrhythmias and cardiac death using adenosine and lidocaine during regional ischemia in the in vivo rat. Am J Physiol Heart Circ Physiol. 2004;287:H1286–95.
19. Plomp TA, Wiersinga WM, Maes RA. Tissue distribution of amiodarone and desethylamiodarone in rats after repeated oral administration of various amiodarone dosages. Arzneimittelforschung. 1985;35:1805–10.
20. Feige JN, Sage D, Wahli W, Desvergne B, Gelman L. PixFRET, an ImageJ plug-in for FRET calculation that can accommodate variations in spectral bleed-trhoughs. Microsc Res Tech. 2005;68:51–8.
21. Opitz CF, Mitchell GF, Pfeffer MA, Pfeffer JM. Arrhythmias and death after coronary artery occlusion in the rat. Continuous telemetric ECG monitoring in conscious, untethered rats. Circulation. 1995;92:253–61.
22. Klibanov AL, Maruyama K, Torchilin VP, Huang L. Amphipathic polyethyleneglycols effectively prolong the circulation time of liposomes. FEBS Lett. 1990;268:235–7.
23. Theodossiou TA, Galanou MC, Paleos CM. Novel amiodarone-doxorubicin cocktail liposomes enhance doxorubicin retention and cytotoxicity in DU145 human prostate carcinoma cells. J Med Chem. 2008;51:6067–74.
24. Elhasi S, Astaneh R, Lavasanifar A. Solubilization of an amphiphilic drug by poly(ethylene oxide)-block-poly(ester) micelles. Eur J Pharm Biopharm. 2007;65:406–13.
25. Kamiya K, Nishiyama A, Yasui K, Hojo M, Sanguinetti MC, Kodama I. Short- and long-term effects of amiodarone on the two components of cardiac delayed rectifier K(+) current. Circulation. 2001;9:1317–24.
26. Kishida S, Nakajima T, Ma J, et al. Amiodarone and N-desethylamiodarone enhance endothelial nitric oxide production in human endothelial cells. Int Heart J. 2006;47:85–93.
27. Ide T, Tsutsui H, Kinugawa S, Utsumi H, Takeshita A. Amiodarone protects cardiac myocytes against oxidative injury by its free radical scavenging action. Circulation. 1999;100:690–2.
28. Freedman MD, Somberg JC. Pharmacology and pharmacokinetics of amiodarone. J Clin Pharamacol. 1991;31:1061–9.
29. Sakamoto J, Miura T, Tsuchida A, Fukuma T, Hasegawa T, Shimamoto K. Reperfusion arrhythmias in the murine heart: their characteristics and alteration after ischemic preconditioning. Basic Res Cardiol. 1999;94:489–95.
30. Tzivoni D, Keren A, Granot H, Gottlieb S, Benhorin J, Stern S. Ventricular fibrillation caused by myocardial reperfusion in Prinzmetal's angina. Am Heart J. 1983;105:323–5.

Journal of Controlled Release 160 (2012) 274–280

Contents lists available at SciVerse ScienceDirect

Journal of Controlled Release

journal homepage: www.elsevier.com/locate/jconrel

Development of anti-HB-EGF immunoliposomes for the treatment of breast cancer

Kaoru Nishikawa [a], Tomohiro Asai [a], Hirokazu Shigematsu [a], Kosuke Shimizu [a], Hisakazu Kato [b], Yoshihiro Asano [b], Seiji Takashima [b], Eisuke Mekada [c], Naoto Oku [a], Tetsuo Minamino [b,*]

[a] Department of Medical Biochemistry and Global COE Program, School of Pharmaceutical Sciences, University of Shizuoka, 52-1 Yada, Suruga-ku, Shizuoka 422-8526, Japan
[b] Department of Cardiovascular Medicine, Osaka University Graduate School of Medicine, Suita, Osaka 565-0871, Japan
[c] Department of Cell Biology, Research Institute for Microbial Diseases, Osaka University, Suita, Osaka 565-0871, Japan

ARTICLE INFO

Article history:
Received 22 August 2011
Accepted 8 October 2011
Available online 14 October 2011

Keywords:
HB-EGF
immunoliposome
breast cancer

ABSTRACT

Increased expression of heparin-binding epidermal growth factor-like growth factor (HB-EGF) is frequently observed in certain cancers such as ovarian and breast cancers, and this protein is a desirable target for drug delivery by a drug delivery system (DDS). In the present study, we developed novel immunoliposomes targeting HB-EGF for cancer therapy. The immunoliposomes significantly associated with Vero-H cells overexpressing HB-EGF compared with their binding to wild-type Vero cells, whereas liposomes without modification by the antibody did not associate with either type of cells. Moreover, enhanced uptake of the immunoliposomes into Vero-H cells was observed as well as that into MDA-MB-231 human breast cancer cells, which are known to highly express HB-EGF. These results suggest that HB-EGF mediates the binding and uptake of the immunoliposomes in HB-EGF-expressing cells. Next, we determined the therapeutic effect of these immunoliposomes encapsulating an anticancer drug on tumor-bearing mice. For this purpose, we prepared doxorubicin (DOX)-encapsulated immunoliposomes and injected them intravenously into mice bearing MDA-MB-231 cancer cells. As a result, these DOX-encapsulated immunoliposomes suppressed not only tumor progression but also tumor regression. In conclusion, our results indicate that anti-HB-EGF antibody-modified liposomes could be a useful DDS carrier for the treatment of HB-EGF-expressing cancers.

1. Introduction

Heparin-binding epidermal growth factor-like growth factor (HB-EGF) is known to stimulate the growth of various cells in an autocrine or a paracrine manner. This protein is highly expressed on various cancer cells, such as those of ovarian and breast cancer [1,2], and is also expressed on tumor angiogenic vessels [3,4]. Therefore, HB-EGF seems to be a target molecule for the treatment of certain cancers. In fact, CRM197, which binds to the EGF-domain of HB-EGF and prevents HB-EGF from binding to ErbB receptors and therefore regulates the cell proliferation, is now under clinical trials [5]. The usefulness of HB-EGF as a molecular target of cancer treatment has been suggested in several reviews [6–8]. Although HB-EGF can be produced as a membrane-anchored form (proHB-EGF) and later processed to its soluble form, a significant amount of proHB-EGF remains on the cell surface [9]. Therefore, HB-EGF might be also a useful target molecule for drug delivery via a DDS to tumors and tumor angiogenic vessels.

In the present study, we aimed at delivering an anticancer drug to HB-EGF-expressing cancer cells by use of liposomes as a drug carrier. Polyethylene glycol (PEG)-modified liposomes have been the most widely investigated as carriers of drugs and molecules having biological activities, since PEG forms an aqueous layer on the liposomal surface that avoids reticuloendothelial system (RES) trapping of the liposomes [10,11]. PEGylated liposomes have a relatively long circulation time and tend to accumulate in tumor tissues through leaky angiogenic vessels, a phenomenon referred to as the enhanced permeability and retention (EPR) effect [12,13]. Moreover, liposomalization can reduce off-target toxicity of the drugs encapsulated [14]. In fact, PEG-modified liposomes containing doxorubicin (DOX) have been used in clinical cancer therapy. On the other hand, actively targeted liposomes decorated with ligands such as antibodies [15,16], proteins such as transferrin [17], and peptides [18–20] achieve more selective drug delivery to tumor tissues. These ligands that recognize tumor- or tumor angiogenic vessel-associated molecules are conjugated to the head of the PEG-chain of liposomes.

Herein, we decorated DOX-loaded liposomes with anti-HB-EGF antibody and evaluated the systemic and targeted delivery of DOX to cancer cells in breast cancer-bearing mice. The results indicate that this immunoliposomal DOX significantly suppressed tumor growth in comparison with non-modified PEG-liposomal DOX. Our findings suggest that targeted delivery of anti-HB-EGF-modified PEGylated liposomes could be a useful carrier of doxorubicin for the treatment of HB-EGF-expressing cancers.

* Corresponding author. Tel.: +81 6 6879 3635; fax: +81 6 6879 3645.
E-mail address: minamino@cardiology.med.osaka-u.ac.jp (T. Minamino).

0168-3659/$ – see front matter © 2011 Elsevier B.V. All rights reserved.
doi:10.1016/j.jconrel.2011.10.010

2. Materials and Methods

2.1. Materials

Anti-human HB-EGF monoclonal antibody (IgG) was ordered and received from Medical and Biological Laboratories Co. Ltd. The monoclonal antibody clone 3E9 specific for HB-EGF was obtained by the method described previously [21]. The 3E9 clone recognized the EGF-like domain of human proHB-EGF, but not that of mouse proHB-EGF. Hydrogenated soy phosphatidylcholine (HSPC), methoxy-polyethyleneglycol 2000-conjugated distearoylphosphatidylethanolamine (DSPE-PEG), and cholesterol were gifts from Nippon Fine Chemical Co. Ltd. (Kobe, Japan). DSPE-PEG-maleimide (SUNBRIGHT DSPE-0.20MA) was obtained from NOF Co. Ltd. (Tokyo, Japan). 1,1'-Dioctadecyl- 3,3,3',3',-tetramethylindocarbocyanine perchlorate ($DiIC_{18}$) was purchased from Molecular Probes, Inc. (Eugene, OR).

2.2. Preparation of Fab' of anti-HB-EGF monoclonal antibody

Stock solution of anti-HB-EGF IgG was applied onto a PD-10 column (GE Healthcare, UK., Ltd., Buckinghamshire) to exchange the solvent for 100 mM sodium citrate buffer, pH 3.5 (100 mg IgG/20 mL). To eliminate the Fc region of the IgG, pepsin (from porcine gastric mucosa, Sigma-Aldrich) solution (final concentration of 0.01% w/v) was added to the antibody solution and incubated the mixture at 37 °C for 3 h, after which the reaction was stopped by the addition of a 10% volume of 3 M Tris–HCl (pH 7.5). The generated $F(ab')_2$ was washed twice with 100 mM sodium phosphate buffer, pH 6.0, and concentrated by ultrafiltration (5,000 *g* for 20 min) with an Amicon® Ultra-4 (10,000 NMWL, Millipore). Ten milligrams aliquot of $F(ab)'_2$ was diluted with 100 mM sodium phosphate buffer, and 0.1 mL of 100 mM cysteamine hydrochloride was added to a final volume of 1 mL, followed by incubation at 37 °C for 90 min. Then, the reaction solution was purified by gel-filtration chromatography (1.0 cm × 50 cm, Ultrogel AcA, PALL Life Sciences), and the Fab' fraction was collected with a fraction collector. The Fab' fraction was concentrated by ultrafiltration (5,000 *g* for 30 min) with Amicon Ultra-4 (10,000 NMWL).

2.3. Preparation of plain liposomes

Liposomes were prepared by thin lipid-film hydration followed by vortexing and sonication. In brief, 20 μmol HSPC and 10 μmol cholesterol dissolved in chloroform were transferred to a round-bottomed flask, evaporated until a thin lipid film had formed on a rotary evaporator under reduced pressure, and stored *in vacuo* for at least 1 h. The dried film was hydrated with 2 mL of saline, warmed at 65 °C in a water bath, vortexed until the lipids had become detached from the side of the flask, and sonicated with a bath-type sonicator at 65 °C. Three cycles of the following were performed: freezing of the liposomal solution in the flask with liquid nitrogen, thawing at room temperature, incubating at 65 °C in a water bath for 5 min, and vortexing for 30 s. Then, the liposomes were filtered through polycarbonate membrane filters having 100-nm-diameter pores by use of an Extruder (Lipex, Vancouver) at 65 °C. Finally, the liposome solution was diluted with saline; and the liposomal pellet was collected after ultracentrifugation (450,000 g × 1 h, CS120GXL, Hitachi) and resuspended in 2 mL of saline.

For the fluorescence-labeling of liposomes, HSPC, cholesterol, and $DiIC_{18}$ (2:1:0.1 as a molar ratio) dissolved in chloroform were used for preparing a thin lipid film. Further preparation was essentially the same as described above except that all procedures were done under shading from ambient light.

For the encapsulation of DOX into the liposomes, the thin lipid film was hydrated in 250 mM ammonium sulfate (pH 5.5) instead of saline; and after freeze-thawing, extrusion for sizing, and centrifugation, the liposomes resuspended in saline was incubated in the presence of 1.8 mg/mL DOX at 65 °C for 1 h. Untrapped DOX was removed by ultracentrifugation, and the liposomal pellet was resusupended in saline (final concentration of 10 mM as DSPC). The encapsulation efficiency of DOX was calculated based on the amount of untrapped DOX and liposomal DOX after the addition of Triton X-100, with DOX quantified at 484-nm absorbance.

2.4. Surface decoration of liposomes with PEG or anti-HB-EGF antibody-PEG

DSPE-PEG (MPEG-2000-DSPE) and DSPE-PEG-maleimide were dissolved in saline to a final concentration of 10 mM each. One milliliter of plain liposomes (10 mM as DSPC) prepared as described above were incubated at 65 °C for 15 min after addition 100 μL of DSPE-PEG or DSPE-PEG-maleimide to obtain PEG-modified liposomes (PEG-Lip) and PEG-maleimide-modified liposomes.

The coupling of Fab' with the maleimide moiety of PEG-maleimide-modified liposomes was performed according to the method described previously [22], with the following modification: Fab' and PEG-maleimide-modified liposomes (1:1 molar ratio of Fab' and maleimide moiety) were mixed, and the coupling reaction was carried out at 4 °C for 20 h. Excess Fab' was separated from the Fab'-coupled liposomes by use of Sepharose 4 Fast Flow gel filtration, and the liposomal fraction was collected. After ultracentrifugation at 450,000 g, 4 °C for 1 h (CS120GXL, Hitachi), the liposomal pellet was resuspended in 1 mL of saline.

Liposome size and ζ-potential were determined with a Zeta Sizer (Nano –ZS, Malvern Instruments, Worcs, UK).

2.5. Cells and cell culture

Vero cells derived from African green monkey's kidney were cultured in MEM medium (GIBCO) supplemented with 10% fetal bovine serum (FBS; Sigma-Aldrich), 100 units/mL penicillin G (MP Biomedicals, Irvine, CA), and 100 μg/mL streptomycin (MP Biomedicals) in a CO_2 incubator. Vero-H cells isolated by transfection with human HB-EGF cDNA [23] were cultured similarly except that the medium was supplemented with 1 μg/mL G418.

MDA-MB-231 human breast cancer cells were cultured in Leibovitz L-15 medium (GIBCO) supplemented with 10% FBS, 100 units/mL penicillin G, and 100 μg/mL streptomycin in a CO_2 incubator.

2.6. Real-time PCR

Vero, Vero-H, and MDA-MB-231 cells were cultured on a 60-mm culture dish for 24 h and washed with ice-cold PBS for three times. Then, the cells were collected by a scraper; and total RNA was extracted with RNeasy Plus Mini Kit (QIAGEN) according to the manufacturer's instruction. Then cDNA was generated from the total RNA samples (4 μg) by using a Ready-To-Go T-Primed First-Strand Kit (GE Healthcare). In the presence of human HB-EGF or β-actin primer (Takara Bio Inc. Shiga, Japan), and SYBR Premix Ex Taq II (Takara Bio), real-time PCR was performed with a Thermal Cycler Dice Real Time System (Takara Bio). The PCR conditions were the following: 95 °C for 30 sec, followed by 40 cycles of 95 °C for 5 sec, 60 °C for 30 sec; 95 °C for 15 sec, 60 °C for 30 sec, and 95 °C for 15 sec.

2.7. Western blotting

Vero, Vero-H, and MDA-MB-231 cells were cultured on a 60-mm culture dish for 24 h and washed with ice-cold PBS for three times. Then, the cells were solubilized in lysis buffer (50 mM Tris–HCl [pH7.4] containing 1% Triton-X, 150 mM NaCl, and protease inhibitors [2 mM PMSF, 50 μg/mL aprotinin, 50 μg/mL pepstatin, and 0.2 mM leupeptin]). The supernatant of the cell lysate was collected and suspended in loading buffer (16 mM Tris–HCl, 2.5% glycerol, 0.5% SDS, 200 mM 2-mercaptoethanol, 0.001% bromophenol blue; pH 6.8).

Immediately after having been heated at 95 °C for 5 min, the sample was subjected to reducing SDS-PAGE on 10% acrylamide gel. Protein concentrations were measured by using a BCA Protein Assay Reagent Kit (PIERCE Biotechnology, Rockford, IL).

After separation by SDS-PAGE, proteins were transferred electrophoretically (40 V, 90 min) to a PVDF membrane (Bio-Rad). After having been blocked with 3% BSA in TBS/Tween 20 buffer (TBS/T: 50 mM Tris HCl [pH 7.4] containing 150 mM NaCl and 0.05% Tween 20), the blots were incubated at 25 °C for 1 h with goat polyclonal anti-HB-EGF antibody (1:2,000 solution, R&D systems) for the detection of HB-EGF. The membrane was washed thrice with TBS/T, and was probed for 60 min at 25 °C with donkey anti-goat horseradish peroxidase-conjugated secondary antibody (1:4,000 dilution). The probed membranes were washed 3 times (10 min each time) with TBS/T, and immunoreactive proteins were detected by using the enhanced chemiluminescence method.

2.8. Binding to and uptake of Ab-PEG-Lip into various cells

Vero, Vero-H, and MDA-MB-231 cells were cultured in a 24-well plate (2×10^4 cells/500 μL/well) at 37 °C for 48 h. After removal of the medium, $DiIC_{18}$-labeled PEG-Lip or Ab-labeled PEG-Lip (0.05 to 0.2 mM as DSPC) was added to the well; and the cells were then incubated at 4 °C or 37 °C. Next, the cells were washed thrice with cold PBS and solubilized with 10 mM Tris buffer, pH 7.4, containing 0.1% SDS. The samples were diluted 200-fold with 10 mM Tris buffer, pH 7.4, containing 0.1% SDS; and aliquots were transferred to a 96-well black plate. The fluorescence intensity was monitored with a multiplate reader (Infinite M200, Tecan), with excitation and emission wave lengths of 549 nm and 592 nm, respectively. The amount of $DiIC_{18}$ associated with the cells was calculated from the standard curve.

2.9. Cell proliferation assay

MDA-MB-231 cells were seeded (2×10^4 cells/well) into a 24-well plate and incubated overnight in a CO_2 incubator. After a change of the medium, the cells were incubated at 37 °C for 4 h in the presence of DOX-encapsulated anti-HB-EGF-decorated immunoliposomes (Ab-PEG-LipDOX), DOX-encapsulated PEG-liposomes (PEG-LipDOX) or free DOX. Then, the viability of the cells was measured with TetraColorOne™ (Seikagaku, Tokyo, Japan) according to the manufacturer's instruction.

2.10. Therapeutic experiment

MDA-MB-231 cells were subcutaneously implanted (8×10^6 cells/0.2 mL/mouse) into 17-week-old BALB/C nu/nu female mice (Japan SLC Inc., Shizuoka, Japan). Then, saline (control), PEG-LipDOX or Ab-PEG-LipDOX was intravenously injected once a week for 3 weeks, on days 14, 21, and day 28 after tumor implantation. The amount of DOX injected was 10 mg/kg each time and; therefore, a total of 30 mg/kg DOX was injected. The tumor size and body weight were monitored daily from day 12 after tumor implantation. Tumor volume was calculated from the following formula:

$$\text{Tumor volume} = 0.4 \times a \times b^2 \quad (a; \text{largest diameter}, b; \text{smallest diameter})$$

The animals were cared for according to the Animal Facility Guidelines of the University of Shizuoka. All animal experiments were approved by the Animal and Ethics Committee of the University of Shizuoka.

Table 1
Particle size and ζ-potential of liposomes.

Liposomes	Size (nm)	ζ-potential (mV)
PEG-Lip	136	-0.03
PEG-LipDOX	139	-3.30
Ab-PEG-Lip	134	-3.02
Ab-PEG-LipDOX	142	-2.94

2.11. Statistical analysis

Differences between groups were evaluated by analysis of variance (ANOVA) with the Tukey *post-hoc* test.

3. Results

3.1. Characterization of Ab-PEG-Lip and Ab-PEG-LipDOX

At first, we examined the characteristics of anti-HB-EGF antibody-modified liposomes (Ab-PEG-Lip) and DOX-loaded Ab-PEG-Lip (Ab-PEG-LipDOX). As shown in Table 1, all liposomal preparations showed similar sizes, about 140 nm, and had almost neutral charges. The efficiency of conjugation of the Fab' fragment of anti-HB-EGF antibody to liposomal PEG-maleimide was determined by the protein amount before and after the conjugation reaction. When 1.94 mg Fab' had been applied on the liposomes, 1.31 mg Fab' was recovered in the

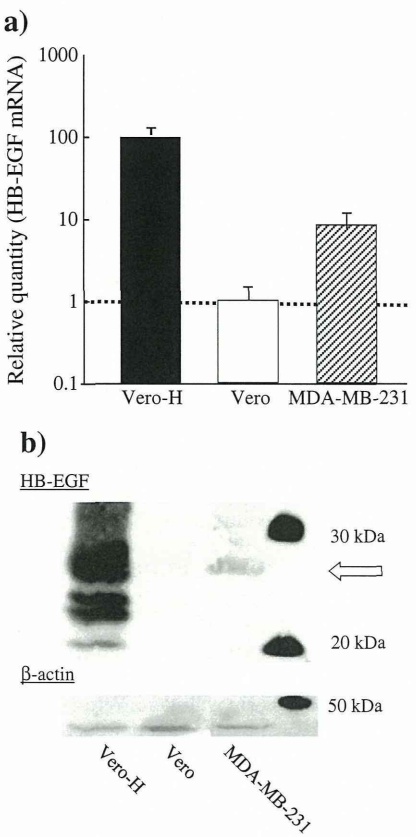

Fig. 1. Expression of HB-EGF and its transcript in various cell lines. a) Relative expression of HB-EGF mRNA was determined by real-time PCR. Total RNA was extracted from Vero, Vero-H, and MDA-MB-231 cells; and then real- time PCR for HB-EGF and β-actin was performed as described in Materials and Methods. b) Western blotting was performed on Vero, Vero-H, and MDA-MB-231 cells. The arrow indicates the position of HB-EGF. Total proteins (14 μg/sample) were fractionated by 10% SDS-PAGE. Following electrophoresis, the proteins were transferred to a PVDF membrane, and Western blotting was performed as described in Materials and Methods.

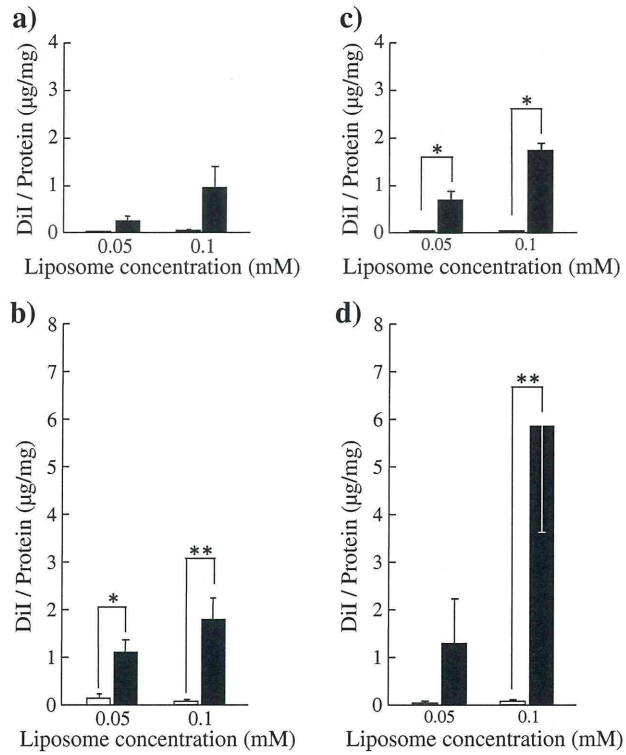

Fig. 2. Binding to and uptake of anti-HB-EGF antibody-modified liposomes into Vero and Vero-H cells. $DiIC_{18}$-labeled PEG-Lip (open columns) and Ab-PEG-Lip (closed columns) were incubated with Vero (a, c) or Vero-H (b, d) cells at 4 °C (a, b) or at 37 °C (c, d) for 4 h. The amount of liposomes bound to Vero or Vero-H cells was determined fluorometrically. Liposomes bound to Vero or Vero-H cells are presented as the amount of $DiIC_{18}$ per amount of cellular protein. Data show the mean values and S.D. (n = 3). Significant differences are shown with asterisks: * $p<0.05$ and ** $p<0.01$, as indicated by the brackets or *versus* corresponding value for PEG-Lip.

liposomal fraction, indicating that the conjugation efficiency was about 67%. The encapsulation efficiency of DOX in PEG-LipDOX and Ab-PEG-LipDOX was 88.2 ± 6.9% and 88.4 ± 4.3%, respectively. These data indicate that the conjugation of Fab' to liposomes and DOX loading were successfully achieved.

3.2. Binding to and uptake of anti-HB-EGF immunoliposomes by HB-EGF-expressing cells

Before examining the cellular-association aspect of Ab-PEG-Lip, we assessed the expression levels of HB-EGF on Vero cells, Vero-H cells, and MDA-MB-231 cells by performing real-time PCR and Western blotting. Quite high expression of HB-EGF on Vero-H cells was confirmed by both real-time PCR (Fig. 1a) and Western blotting (Fig. 1b). Also, substantial amounts of HB-EGF mRNA and protein were expressed on MDA-MB-231 cells. In the case of Vero cells, the expression level of HB-EGF mRNA was about 100-fold less than that in Vero-H cells; and only a light band was detected by Western blotting.

The association of Ab-PEG-Lip with Vero, Vero-H, and MDA-MB-231 cells was examined for evaluating the targeting effectiveness of the liposomes. Ab-PEG-Lip bound more to Vero-H cells than to Vero cells (Fig. 2a, b). Moreover, the amount of the immunoliposomes taken up into cells was greater for Vero-H cells than for Vero cells. Most of the liposome-associated label (DiI) had probably been taken up into the cells at 37 °C, although some of it may have remained bound to the surface of the cells.

Next the uptake of Ab-PEG-Lip into human breast cancer cells was investigated by using MDA-MB-231 cells, which had been confirmed by real-time PCR and Western blotting (Fig. 1) to have high expression of HB-EGF protein. Ab-PEG-Lip was significantly taken up into the MDA-MB-231 cells at 37 °C(Fig. 3). These data would also include the liposomes bound to the cells. Therefore, these immunoliposomes bound to and were taken up specifically into the HB-EGF-expressing breast-cancer cells, indicating that they could be a useful carrier for drug delivery.

3.3. Antiproliferative effect of DOX encapsulated in anti-HB-EGF immunoliposomes on HB-EGF-expressing cells

Next, the anti-proliferative effect of DOX encapsulated in Ab-PEG-Lip on MDA-MB-231 cells as well as on Vero-H cells was examined. As shown in Fig. 4, the immunoliposomal formulation of DOX suppressed the growth of both MDA-MB-231 and Vero-H cells in a

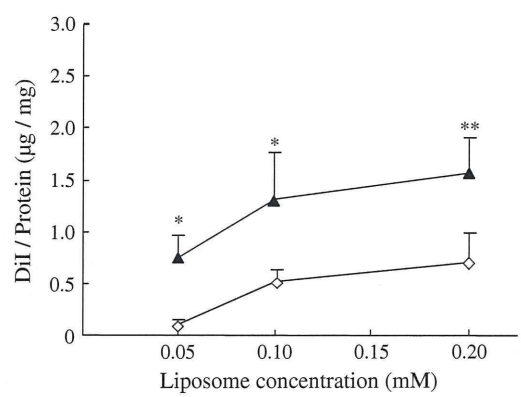

Fig. 3. Association of anti-HB-EGF antibody-modified liposomes with MDA-MB-231 cells. MDA-MB-231 cells were incubated with $DiIC_{18}$-labeled PEG-Lip (◇) or Ab-PEG-Lip (▲) at 37 °C for 4 h. After the cells had been washed with PBS, the amount of liposomes associated with them was determined fluorometrically. Amounts of bound/internalized liposomes are presented as the amount of $DiIC_{18}$ per amount of MDA-MB-231 cell protein. Data show the mean values and S.D. (n = 3). Significant differences are shown with asterisks: * $p<0.05$ and ** $p<0.01$ *versus* corresponding value for PEG-Lip.

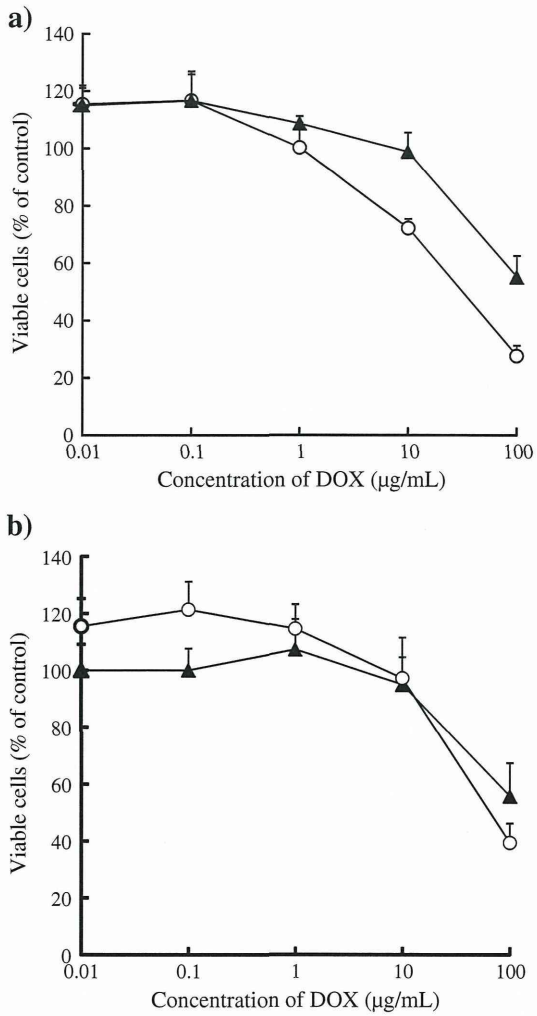

Fig. 4. Anti-proliferative effect of Ab-PEG-LipDOX on Vero-H and MDA-MB-231 cells. Vero-H (a) or MDA-MB-231(b) cells (2.5 x 10^3 cells/well) were seeded into a 96-well plate. Ab-PEG-LipDOX (▲) or free DOX (○) was added at the indicated concentrations (0.01, 0.1, 1, 10, and 100 μg/mL as DOX), and the cells were then incubated for 4 h at 37 °C. After having been washed with PBS, the cells were cultured in fresh medium for an additional 48 h at 37 °C. TetraColor ONE™ was then added to each well. After a 3-h incubation, the absorbance at 450 nm was measured. Data (n = 4) are presented as the percentage (mean and S.D.) of viable cells relative to the control (taken as 100%) at the indicated DOX dosages.

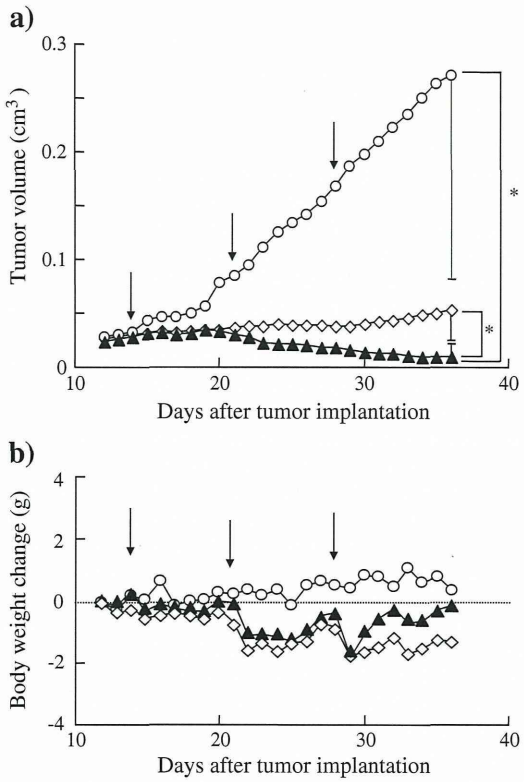

Fig. 5. Suppression of tumor growth in MDA-MB-231 carcinoma-bearing mice treated with Ab-PEG-LipDOX. BALB/C nu/nu female mice (n = 5) were implanted subcutaneously with MDA-MB-231 carcinoma into the left posterior flank. At 14, 21, and 28 days after tumor implantation, they were injected intravenously with PEG-LipDOX (◇), Ab-PEG-LipDOX (▲) or saline (○). The injected dose of liposomal DOX was 10 mg/kg as DOX for each administration. Tumor volume (a) and change in body weight (b) of the tumor-bearing mice were monitored daily after day 12. Data in "a" are presented as the mean tumor volume and S.D., where the S.D. bars are shown only for the last points for the sake of graphic clarity. Arrows show the day of treatment. Asterisks indicate a significant difference: * $p<0.05$, as indicated by the brackets.

dose-dependent manner. Although free DOX suppressed the growth of both types of cells a little stronger than liposomal DOX, Ab-PEG-LipDOX might be expected to be effective *in vivo*. Since PEG-Lip did not show comparable association with the cells, we did not examine the effect of DOX encapsulated in PEG-Lip.

3.4. Therapeutic efficacy of DOX encapsulated in anti-HB-EGF immunoliposomes on MDA-MB-231 tumor-bearing mice

Finally, the therapeutic effect of DOX-encapsulated immunoliposomes on MDA-MB-231 solid tumors implanted subcutaneously into mice was examined. As shown in Fig. 5, both PEG-LipDOX and Ab-PEG-LipDOX strongly suppressed the tumor growth when give as 3 doses of 10 mg/kg DOX. Free DOX of this amount could not be injected due to the severe side effects. Between liposomal DOX-treated groups, PEG-LipDOX-treated group showed only a little tumor growth and the Ab-PEG-LipDOS-treated group showed tumor regression. The change in body weight was monitored as an indicator of side effects, and a decrease in body weight was observed in both liposomal DOX-treated groups. This decrease, however, was not so much; and the body weight recovered at least by a week after the last treatment (Fig. 5b).

4. Discussion

In spite of diagnostic and therapeutic advances, cancer is still the leading cause of death in many countries. The present study focused on the treatment of human cancers by use of a HB-EGF-targeted liposomal drug delivery system, since various cancerous cells are known to frequently express this protein. For this purpose, we developed anti-HB-EGF antibody-decorated PEG liposomes encapsulating DOX. In this study, we used Fab' antibody instead of IgG, since removal of the Fc region endows antibody-decorated liposomes with a relatively long circulation time in the bloodstream by avoiding RES trapping [24]. In the present protocol, the efficiency of Fab' conjugation to the liposomal surface was about 70%, which amount was calculated to represent about 120 μg protein/μmol lipids. Since about 30 μg Fab'/μmol lipids is reported to be necessary for the function of immunoliposomes [25,26], the Ab-PEG-Lip prepared presently displayed a sufficient amount of Fab'. The size of liposomes is another important factor for deciding the pharmacokinetics of the liposomes, and about 140-nm liposomes are considered desirable for their accumulation in tumor tissue by the EPR effect [27].

Firstly the expression of HB-EGF in Vero, Vero-H, and MDA-MB-231 cells was examined at mRNA and protein levels. Extremely high expression of HB-EGF was observed in Vero-H cells that had been

constructed for overexpressing human HB-EGF. Vero cells, which are non-cancerous normal cells originally isolated from an African green monkey, also expressed HB-EGF; although the mRNA expression level was about 100-fold less than that of Vero-H cells, and 10-fold less than that of MDA-MB-231 cells. Since the anti-human HB-EGF antibody used for Western blotting is known to cross react with monkey HB-EGF, an HB-EGF band was detected in Vero cells.

By use of these cells, we determined the binding to and uptake of Ab-EGF-Lip into the cells. The cell-associated liposomes detected after incubation at 4 °C might have been mainly due to liposomes bound on the surface of the cells, whereas those detected after incubation at 37 °C would have included both bound and internalized liposomes. The binding of Ab-EGF-Lip to Vero H and MDA-MB-231 cells was very obvious compared with that to Vero cells, although Ab-EGF-Lip also bound to Vero cells to some extent. This finding suggests that the expression of endogenous HB-EGF in Vero cells was adequate for binding of the liposomes to some extent. Alternatively, part of the binding might be explained by non-specific binding of Ab-EGF-Lip via the Fab' despite its specificity. Since PEG-Lip showed little association with those cells, the anti-HB-EGF Fab'-decoration could have been responsible for the increased association of Ab-EGF-Lip with them.

DOX encapsulation into Ab-PEG-Lip was performed by the remote loading method using ammonium sulfate, since this method enables stable entrapment of DOX in the internal aqueous phase of PEG-liposomes [28] and immunoliposomes [29]. When the antiproliferative effect of Ab-PEG-LipDOX was examined, the cytotoxicity of Ab-PEG-LipDOX against Vero-H and MDA-MB-231 cells was found to be comparable to that of free DOX.

Finally, we performed a therapeutic experiment by use of MDA-MB-231 breast cancer cell-bearing mice. Both PEG-LipDOX and Ab-PEG-LipDOX strongly suppressed tumor growth. PEG-liposomes are known to accumulate in tumor tissues due to the EPR effect. Since this effect in tumor tissues is based on the leaky angiogenic vessels, hyper vascular tumors such as breast and ovarian tumors are desired targets. Therefore, PEG-liposomes encapsulating DOX were originally used for the treatment of ovarian and breast cancers and of HIV-associated Kaposi's sarcoma. The strong *in vivo* therapeutic effect of PEG-LipDOX against MDA-MB-231 tumors observed in this study is thus reasonable. Moreover, Ab-PEG-LipDOX, having both passive and active targeting characteristics, showed a stronger therapeutic effect against MDA-MB-231 tumors than PEG-LipDOX. PEG-liposomes that accumulate in tumor tissues after an intravenous injection are thought to reside mainly in the interstitial spaces in the tumor. On the other hand, decoration of them with some specific probes may alter the intratumoral distribution of the liposomes, and increase the uptake of liposomal drugs into the target cells, as observed in the present study.

As shown in Fig. 5, tumor growth inhibition was similar in both PEG-LipDOX- and Ab-PEG-LipDOX-treated groups until day 20, and differential therapeutic effect between targeted and non-targeted liposomes became obvious after second and third injection of them. We do not know the reason why the advantage of immunoliposomes was not obvious until day 20 at present. One possible explanation is as follows: The growth of MDA-MB-231 cells in vivo was not so fast, and the tumor mass was quite small at the first injection time, namely day 14. Therefore, the angiogenesis that produced leaky endothelium did not hardly occur. Moreover immune system would be still quite active that eliminate even PEGylated liposomes at this stage. In fact, although both PEG-LipDOX and Ab-PEG-LipDOX suppressed tumor growth to some extent compared to control, body weight change was not so obvious compared to that after second and third injection. At the time of second and third injection, immune systems were weakened because of tumor residing that helps the accumulation of liposomes in the tumor by EPR effect through neovessels. Since extravasation by EPR effect is prerequisite for the active targeting of immunoliposomes to the tumor cells, Ab-PEG-LipDOX thus accumulated in the interstitial space of the tumor interacted with tumor cells and produced higher therapeutic effect than PEG-LipDOX. Actually, tumor was hardly palpated in two mice out of five after the third treatment with Ab-PEG-LipDOX.

5. Conclusions

For the purpose of active targeting of anticancer drugs to cancer cells, anti-HB-EGF antibody-decorated liposomes were prepared. These immunoliposomes bound to and were taken up into not only Vero-H cells highly expressing HB-EGF but also MDA-MB-231 human breast cancer cells. Moreover, DOX-encapsulated, anti-HB-EGF antibody-decorated liposomes caused strong suppression and regression of MDA-MB-231 tumors in mice. These results indicate that anti-HB-EGF antibody-decorated liposomes could be a useful DDS carrier for the treatment of HB-EGF-expressing cancers.

References

[1] S. Miyamoto, M. Hirata, A. Yamazaki, T. Kageyama, H. Hasuwa, H. Mizushima, Y. Tanaka, H. Yagi, K. Sonoda, M. Kai, H. Kanoh, H. Nakano, E. Mekada, Heparin-binding EGF-like growth factor is a promising target for ovarian cancer therapy, Cancer Res. 64 (2004) 5720–5727.

[2] S. Miyamoto, H. Yagi, F Yotsumoto, S. Horiuchi, T. Yoshizato, T. Kawarabayashi, M. Kuroki, E. Mekada, New approach to cancer therapy: heparin binding-epidermal growth factor-like growth factor as a novel targeting molecule, Anticancer Res. 27 (2007) 3713–3721.

[3] P.P. Ongusaha, J.C. Kwak, A.J. Zwible, S. Macip, S. Higashiyama, N. Taniguchi, L. Fang, S.W. Lee, HB-EGF is a potent inducer of tumor growth and angiogenesis, Cancer Res. 64 (2004) 5283–5290.

[4] V.B. Mehta, G.E. Besner, HB-EGF promotes angiogenesis in endothelial cells via PI3-kinase and MAPK signaling pathways, Growth Factors 25 (2007) 253–263.

[5] S. Miyamoto, H. Yagi, F. Yotsumoto, T. Kawarabayashi, E. Mekada, Heparin-binding epidermal growth factor-like growth factor as a novel targeting molecule for cancer therapy, Cancer Sci. 97 (2006) 341–347.

[6] S. Miyamoto, T. Fukami, H. Yagi, M. Kuroki, F. Yotsumoto, Potential for molecularly targeted therapy against epidermal growth factor receptor ligands, Anticancer Res. 29 (2009) 823–830.

[7] H. Tsujioka, F. Yotsumoto, K. Shirota, S. Horiuchi, T. Yoshizato, M. Kuroki, S. Miyamoto, Emerging strategies for ErbB ligand-based targeted therapy for cancer, Anticancer Res. 30 (2010) 3107–3112.

[8] H. Tsujioka, F. Yotsumoto, S. Hikita, T. Ueda, M. Kuroki, S. Miyamoto, Targeting the heparin-binding epidermal growth factor-like growth factor in ovarian cancer therapy, Curr. Opin. Obstet. Gynecol. 23 (2011) 24–30.

[9] S. Higashiyama, H. Iwabuki, C. Morimoto, M. Hieda, H. Inoue, N. Matsushita, Membrane-anchored growth factors, the epidermal growth factor family: beyond receptor ligands, Cancer Sci. 99 (2008) 214–220.

[10] D.D. Lasic, Doxorubicin in sterically stabilized liposomes, Nature 380 (1996) 561–562.

[11] Y. Sadzuka, A. Nakade, R. Hirama, A. Miyagishima, Y. Nozawa, S. Hirota, T. Sonobe, Effects of mixed polyethyleneglycol modification on fixed aqueous layer thickness and antitumor activity of doxorubicin containing liposome, Int. J. Pharm. 238 (2002) 171–180.

[12] Y. Matsumura, H. Maeda, A new concept for macromolecular therapeutics in cancer chemotherapy: mechanism of tumoritropic accumulation of proteins and the antitumor agent smancs, Cancer Res. 46 (1986) 6387–6392.

[13] H. Maeda, Y. Matsumura, EPR effect based drug design and clinical outlook for enhanced cancer chemotherapy, Adv. Drug Deliv. Rev. 63 (2011) 129–130.

[14] A. Gabizon, H. Shmeeda, Y. Barenholz, Pharmacokinetics of pegylated liposomal doxorubicin: review of animal and human studies, Clin. Pharmacokinet. 42 (2003) 419–436.

[15] A.S. Manjappa, K.R. Chaudhari, M.P. Venkataraju, P. Dantuluri, B. Nanda, C. Sidda, K.K. Sawant, R.S. Murthy, Antibody derivatization and conjugation strategies: application in preparation of stealth immunoliposome to target chemotherapeutics to tumor, J. Control. Release 150 (2011) 2–22.

[16] K. Atobe, T. Ishida, E. Ishida, K. Hashimoto, H. Kobayashi, J. Yasuda, T. Aoki, K. Obata, H. Kikuchi, H. Akita, T. Asai, H. Harashima, N. Oku, H. Kiwada, In vitro efficacy of a sterically stabilized immunoliposomes targeted to membrane type 1 matrix metalloproteinase (MT1-MMP), Biol. Pharm. Bull. 30 (2007) 972–978.

[17] R. Suzuki, T. Takizawa, Y. Kuwata, M. Mutoh, N. Ishiguro, N. Utoguchi, A. Shinohara, M. Eriguchi, H. Yanagie, K. Maruyama, Effective anti-tumor activity of oxaliplatin encapsulated in transferrin-PEG-liposome, Int. J. Pharm. 346 (2008) 143–150.

[18] N. Maeda, Y. Takeuchi, M. Takada, Y. Sadzuka, Y. Namba, N. Oku, N, Anti-neovascular therapy by use of tumor neovasculature-targeted long-circulating liposome, J. Control. Release 100 (2004) 41–52.

[19] Y. Katanasaka, T. Ida, T.T. Asai, N. Maeda, N. Oku, Effective delivery of an angiogenesis inhibitor by neovessel-targeted liposomes, Int. J. Pharm. 360 (2008) 219–224.